THE JOURNAL OF BIOLOGICAL CHEMISTRY VOL. 284, NO. 37, pp. 25190–25198, September 11, 2009
© 2009 by The American Society for Biochemistry and Molecular Biology, Inc. Printed in the U.S.A.

Roles of Interaction between Actuator and Nucleotide Binding Domains of Sarco(endo)plasmic Reticulum Ca^{2+}-ATPase as Revealed by Single and Swap Mutational Analyses of Serine 186 and Glutamate 439*[S]

Received for publication, June 15, 2009, and in revised form, July 3, 2009 Published, JBC Papers in Press, July 23, 2009, DOI 10.1074/jbc.M109.034140

Xiaoyu Liu, Takashi Daiho, Kazuo Yamasaki, Guoli Wang, Stefania Danko, and Hiroshi Suzuki[1]

From the Department of Biochemistry, Asahikawa Medical College, Asahikawa 078-8510, Japan

Roles of hydrogen bonding interaction between Ser^{186} of the actuator (A) domain and Glu^{439} of nucleotide binding (N) domain seen in the structures of ADP-insensitive phosphorylated intermediate (*E*2P) of sarco(endo)plasmic reticulum Ca^{2+}-ATPase were explored by their double alanine substitution S186A/E439A, swap substitution S186E/E439S, and each of these single substitutions. All the mutants except the swap mutant S186E/E439S showed markedly reduced Ca^{2+}-ATPase activity, and S186E/E439S restored completely the wild-type activity. In all the mutants except S186E/E439S, the isomerization of ADP-sensitive phosphorylated intermediate (*E*1P) to *E*2P was markedly retarded, and the *E*2P hydrolysis was largely accelerated, whereas S186E/E439S restored almost the wild-type rates. Results showed that the Ser^{186}-Glu^{439} hydrogen bond stabilizes the *E*2P ground state structure. The modulatory ATP binding at sub-mM~mM range largely accelerated the *E*P isomerization in all the alanine mutants and E439S. In S186E, this acceleration as well as the acceleration of the ATPase activity was almost completely abolished, whereas the swap mutation S186E/E439S restored the modulatory ATP acceleration with a much higher ATP affinity than the wild type. Results indicated that Ser^{186} and Glu^{439} are closely located to the modulatory ATP binding site for the *E*P isomerization, and that their hydrogen bond fixes their side chain configurations thereby adjusts properly the modulatory ATP affinity to respond to the cellular ATP level.

Sarcoplasmic reticulum Ca^{2+}-ATPase (SERCA1a)[2] is a representative member of P-type ion-transporting ATPases and catalyzes Ca^{2+} transport coupled with ATP hydrolysis (Fig. 1) (1–9). In the catalytic cycle, the enzyme is activated by binding of two Ca^{2+} ions at the transport sites (*E*2 to *E*1Ca_2, steps 1–2) and then autophosphorylated at Asp^{351} with MgATP to form ADP-sensitive phosphoenzyme (*E*1P, step 3), which can react with ADP to regenerate ATP. Upon formation of this *E*P, the bound Ca^{2+} ions are occluded in the transport sites (*E*1PCa_2). The subsequent isomeric transition to ADP-insensitive form (*E*2P) results in a change in the orientation of the Ca^{2+} binding sites and reduction of their affinity, and thus Ca^{2+} release into lumen (steps 4 and 5). Finally, the hydrolysis takes place and returns the enzyme into an unphosphorylated and Ca^{2+}-unbound form (*E*2, step 6). *E*2P can also be formed from P_i in the presence of Mg^{2+} and the absence of Ca^{2+} by reversal of its hydrolysis.

The cytoplasmic three domains N, A, and P largely move and change their organization states during the Ca^{2+} transport cycle (10–22). These changes are linked with the rearrangements in the transmembrane helices. In the *E*P isomerization (loss of ADP sensitivity) and Ca^{2+} release, the A domain largely rotates (by ~110° parallel to membrane plane), intrudes into the space between the N and P domains, and the P domain largely inclines toward the A domain. Thus in *E*2P, these domains produce the most compactly organized state (see Fig. 2 for the change $E1Ca_2{\cdot}AlF_4^-{\cdot}ADP \rightarrow E2{\cdot}MgF_4^{2-}$ as the model for the overall process $E1PCa_2{\cdot}ADP^{\ddagger} \rightarrow E2{\cdot}P_i$).

We have found that the interactions between the A and P domains at the Val^{200}-loop (Asp^{196}-Asp^{203}) with the residues of the P domain (Arg^{678}/Glu^{680}/Arg^{656}/Asp^{660}) (23) and at the Tyr^{122} hydrophobic cluster (24–26) (see Fig. 2) play critical roles for Ca^{2+} deocclusion/release in $E2PCa_2 \rightarrow E2P + 2Ca^{2+}$ after the loss of ADP sensitivity (*E*1PCa_2 to *E*2PCa_2 isomerization). The proper length of the A/M1′ linker is critical for inducing the inclining motion of the A and P domains for the Ca^{2+} deocclusion and release from *E*2PCa_2 (27, 28). The importance of the interdomain interaction between Arg^{678} (P) and Asp^{203} (A) in stabilizing the *E*2P and *E*2 intermediates and its influence on modulatory ATP activation were pointed out by the mutation R678A (29). Regarding the N domain, the importance of Glu^{439} in the *E*P isomerization and *E*2P hydrolysis was previously noted by its alanine substitution, and possible importance of its interaction with Ser^{186} on the A domain has been suggested since Glu^{439} forms a hydrogen bond with Ser^{186} in the *E*2P analog structures (29) (see Fig. 2). The Darier disease-causing mutations of Ser^{186} of SERCA2b, S186P and S186F also alter the kinetics of the *E*P processing and its impor-

* This work was supported by a grant-in-aid for scientific research (B) (to H. S.) from the Ministry of Education, Culture, Sports, Science and Technology of Japan.

[S] The on-line version of this article (available at http://www.jbc.org) contains supplemental Figs. S1–S3.

[1] To whom correspondence should be addressed: Dept. of Biochemistry, Asahikawa Medical College, Midorigaoka-Higashi, Asahikawa, 078-8510, Japan. Tel.: 81-166-68-2350; Fax: 81-166-68-2359; E-mail: hisuzuki@asahikawa-med.ac.jp.

[2] The abbreviations used are: SERCA1a, adult fast-twitch skeletal muscle sarcoplasmic reticulum Ca^{2+}-ATPase; *E*P, phosphoenzyme; *E*1P, ADP-sensitive phosphoenzyme; *E*2P, ADP-insensitive phosphoenzyme; MOPS, 3-(*N*-morpholino)propanesulfonic acid; TG, thapsigargin; PDB, Protein Data Bank; A, actuator domain; N, nucleotide binding domain; P, phosphorylation domain.

tance as the residue in the immediate vicinity of TGES^{184} has been pointed out (30, 31). Notably also, Glu^{439} is situated near the adenine binding pocket and its importance in the ATP binding and ATP-induced structural change have been shown (32, 33). In the structure *E*2(TG)AMPPCP (*E*2·ATP), Glu^{439} interacts with the modulatory ATP binding via Mg^{2+}, and is involved in the acceleration of the Ca^{2+}-ATPase cycle (16).

Considering these critical findings on each of Glu^{439} and Ser^{186}, it is crucial to reveal the role of the Ser^{186}-Glu^{439} hydrogen-bonding interaction between the A and N domains in the *E*P processing and its ATP modulation (*i.e.* regulatory ATP-induced acceleration). We therefore made a series of mutants on both Ser^{186} and Glu^{439} including the swap substitution mutant, S186A, E439A, S186A/E439A, S186E, E439S, S186E/E439S, and explored their kinetic properties. Results showed that the Ser^{186}-Glu^{439} hydrogen bond is critical for the stabilization of the *E*2P ground state structure, and possibly functioning as to make the *E*2P resident time long enough for Ca^{2+} release ($E2PCa_2 \rightarrow E2P + 2Ca^{2+}$) thus to avoid its hydrolysis without Ca^{2+} release. Results also revealed that the side-chain configurations of Ser^{186} and Glu^{439} are fixed by their hydrogen bond, thereby conferring the proper modulatory ATP binding to occur at the cellular ATP level to accelerate the rate-limiting *E*P isomerization.

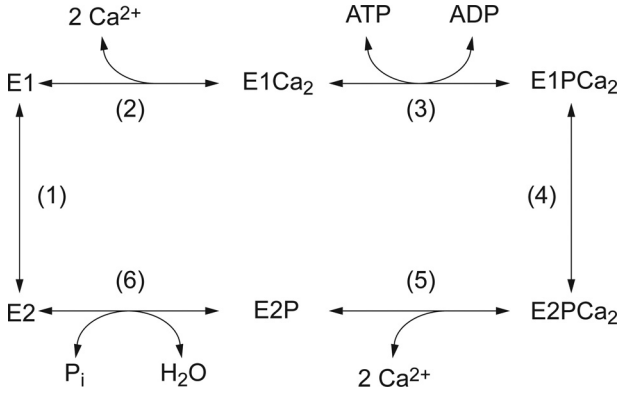

FIGURE 1. **Reaction cycle of sarco(endo)plasmic reticulum Ca^{2+}-ATPase.**

EXPERIMENTAL PROCEDURES

Mutagenesis and Expression—The Stratagene QuikChange™ site-directed mutagenesis method (Stratagene, La Jolla, CA) was utilized for the substitution in the rabbit SERCA1a cDNA. The ApaI-KpnI or KpnI-SalI restriction fragments with the desired mutation were excised from the plasmid and ligated back into the corresponding region in the full-length SERCA1a cDNA in the pMT2 expression vector (34). The pMT2 DNA was transfected into COS-1 cells by the liposome-mediated transfection method. Microsomes were prepared from the cells as described (35). "Control microsomes" were prepared from COS-1 cells transfected with the pMT2 vector containing no SERCA1a cDNA. The amount of expressed SERCA1a was quantified by immunosorbent assay (36). Expression levels of wild-type SERCA1a and the mutants were 2–3% of total microsomal proteins.

Ca^{2+}-ATPase Activity—The rate of ATP hydrolysis was determined at 25 °C with 20 μg/ml microsomal protein in various concentrations of ATP, 1 μM A23187, 0.1 M KCl, 7 mM $MgCl_2$, 0.05 mM $CaCl_2$, or 5 mM EGTA, and 50 mM MOPS/Tris (pH 7.0), otherwise as noted in the legends for figures. The Ca^{2+}-ATPase activity of the expressed SERCA1a of the microsomes was obtained by subtracting the Ca^{2+}-ATPase activity of the control microsome.

Formation and Hydrolysis of EP—Phosphorylation of SERCA1a in microsomes with [γ-^{32}P]ATP or $^{32}P_i$, and dephosphorylation of ^{32}P-labeled SERCA1a were performed as described in the legends to figures. The reactions were quenched with ice-cold trichloroacetic acid

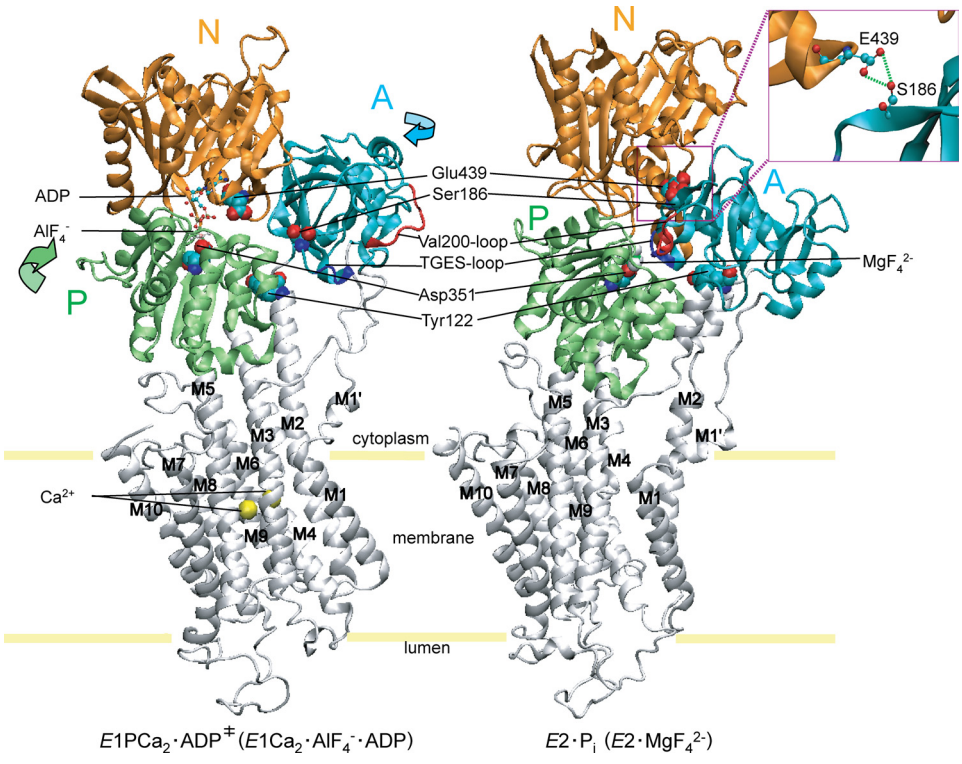

FIGURE 2. **Structure of SERCA1a and formation of Ser^{186}-Glu^{439} hydrogen bond between the A and N domains.** The coordinates for the structures $E1Ca_2$·AlF_4^-·ADP, (the analog for the transition state of the phosphoryl transfer $E1PCa_2$·ADP‡, *left panel*) and E2·MgF_4^{2-} (*E*2·P_i analog (21), *right panel*) of Ca^{2+}-ATPase were obtained from the Protein Data Bank (PDB accession code 1T5T and 1WPG, respectively (12, 14)). The *arrows* indicate approximate movements of the A and P domains in the change from $E1Ca_2$·AlF_4^-·ADP to E2·MgF_4^{2-}. Ser^{186} and Glu^{439} are depicted as van der Waals spheres. These two residues form a hydrogen bond in E2·MgF_4^{2-} (see *inset*). The phosphorylation site Asp^{351}, two Ca^{2+} at the transport sites and ADP with AlF_4^- at the catalytic site in $E1Ca_2$·AlF_4^-·ADP, MgF_4^{2-} bound at the catalytic site in E2·MgF_4^{2-} are depicted. The TGES^{184} loop and Val^{200} loop of the A domain and Tyr^{122} on the *top part* of M2 are shown. These elements produce three interaction networks between A and P domains and M2 (Tyr^{122}) in E2·MgF_4^{2-} (23–26). M1′ and M1-M10 are also indicated.

containing P_i. Rapid kinetics measurements were performed with a handmade rapid mixing apparatus (37). The precipitated proteins were separated by 5% SDS-PAGE at pH 6.0 according to Weber and Osborn (38). The radioactivity associated with the separated Ca^{2+}-ATPase was quantitated by digital autoradiography (39). The amount of *E*P formed with the expressed SERCA1a was obtained by subtracting the background radioactivity with the control microsomes, which was less than 5% of the radioactivity of *E*P of the expressed wild-type SERCA1a.

Miscellaneous—Protein concentrations were determined by the method of Lowry *et al.* (40) with bovine serum albumin as a standard. Data were analyzed by nonlinear regression using the program Origin (Microcal Software, Inc., Northampton, MA). The concentrations of free Ca^{2+}, Mg^{2+}, ATP, and MgATP were calculated by Calcon program. Three-dimensional models of the enzyme were reproduced by the program VMD (41).

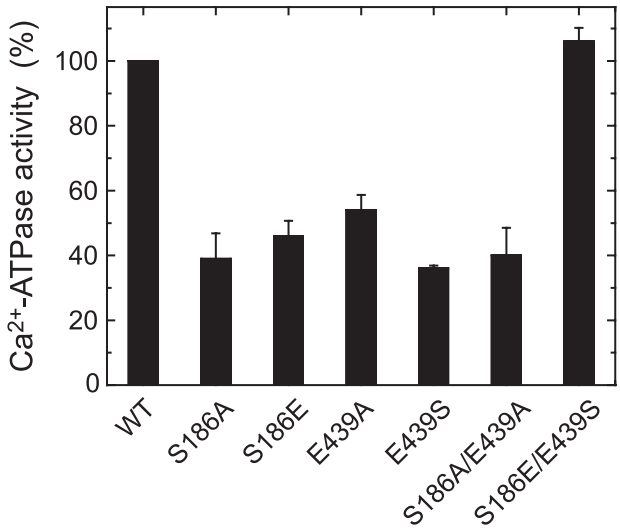

FIGURE 3. **Ca^{2+}-ATPase activities of expressed SERCA1a.** The Ca^{2+}-ATPase activity of microsomes expressing the wild-type or mutant SERCA1a was determined with 0.1 mM [γ-^{32}P]ATP as described under "Experimental Procedures." The activities are divided by the amount of *E*P formed at steady state (see supplemental Fig. S1), and the turnover rates thus obtained are shown as percentage of that of the wild type (7.29 ± 0.42 s^{-1} (n = 5)). The values of the mutants presented are the mean ± S.D. (n = 3–5).

RESULTS

Ca^{2+}-ATPase Activity—All the mutants S186A, S186E, E439A, E439S, S186A/E439A, and S186E/E439S were expressed in COS-1 cells at the levels comparable to the wild type. The amounts of *E*P formed with ATP at a saturating 50 μM Ca^{2+} in the mutants were comparable to the wild type (see the maximum levels in supplemental Fig. S1). In Fig. 3, the Ca^{2+}-ATPase activities of the mutants and wild type in the microsomes were determined at 0.1 mM MgATP, and the turnover rate was calculated by dividing the activity with the amount of maximum *E*P. The mutations S186A, S186E, E439A, E439S, and S186A/E439A caused significant reduction of the activity, whereas the swap mutation S186E/E439S completely restored the wild-type activity. The result for E439A agrees with the previous finding by Clausen *et al.* (29).

Ca^{2+} Affinity and E2 to E1Ca$_2$ Transition—The Ca^{2+} affinities at the transport sites estimated by the activation of *E*P formation were nearly the same in all the mutants as in the wild type (Table 1 and supplemental Fig. S2). The rates of the *E*2 to *E*1Ca$_2$ transition were then determined at pH 6 where the equilibrium between *E*1 and *E*2 in the absence of Ca^{2+} is most shifted to *E*2 (42). In this experiment, the enzyme was first preincubated without Ca^{2+} and then phosphorylated by simultaneous addition of saturating Ca^{2+} and ATP. The time courses of *E*P formation were well described by first-order kinetics (supplemental Fig. S1), and the rates obtained are listed in Table 1. When ATP was added to the enzyme preincubated with Ca^{2+} (*E*1Ca$_2$) otherwise as above, the *E*P formation was much faster and completed within ~1 s; therefore, the rates obtained above reflect the rate-limiting *E*2 to *E*1Ca$_2$ transition. The substitutions of Ser^{186} and Glu^{439} did not give much changes, although S186E/E439S somewhat increased the rate.

E1PCa$_2$ to E2P Isomerization and Decay of E1PCa$_2$ Formed from ATP—In Fig. 4, the accumulation of ADP-insensitive *E*P (*E*2P) in the presence and absence of K^+ was determined at 0 °C and at 15 s (nearly the steady state) after addition of 10 μM ATP. In the presence of K^+, which strongly accelerates the hydrolysis of *E*2P and thus suppresses its accumulation in the wild type (43, 44), the fraction of accumulated *E*2P in all the mutants was very low as in the wild type. In the absence of K^+, the *E*2P

TABLE 1

Kinetic parameters determined for partial reaction steps

The affinity of the transport sites for Ca^{2+} was estimated in supplemental Fig. S2 as the Ca^{2+}-induced activation of *E*P formation, and the $K_{0.5}$ value and Hill coefficient (n_H) are shown. The rate of the *E*2 to *E*1Ca$_2$ transition in steps 1–2 were determined by the *E*1PCa$_2$ formation from the *E*2 state (*i.e.* the rate-limiting *E*2 to *E*1Ca$_2$ transition in steps 1–2) upon the simultaneous addition of saturating 100 μM Ca^{2+} and ATP in supplemental Fig. S1. The rates in the other steps were obtained in Fig. 5 (loss of ADP sensitivity in steps 4–5 in the absence of K^+), Fig. 6 (decay of *E*1PCa$_2$ formed from ATP in the presence of Ca^{2+} (*EP*$_{ATP}$), *i.e.* rate-limiting *E*1PCa$_2$ to *E*2P isomerization in steps 4–5 in 0.1 M K^+), and Fig. 7 (hydrolysis of *E*2P formed from P_i in the absence of Ca^{2+} (*E*2P$_{Pi}$) in step 6). The concentrations of BeF_3^- and AlF_4^- ($K_{0.5}$) giving the half-maximum formation of *E*2·BeF_3^- and *E*2·AlF_4^- from the *E*2 state were obtained in supplemental Fig. S3.

	Affinity for Ca^{2+}		*E*2 to *E*1Ca$_2$		Loss of ADP sensitivity		Decay of *EP*$_{ATP}$[a]		Hydrolysis of *E*2P$_{Pi}$		$K_{0.5}$ in formation of *E*2P analog			
	$K_{0.5}$	n_H			(−)K^+		(+)K^+		(+)K^+		BeF_3^-		AlF_4^-	
	μM		s^{-1}	(%)	s^{-1}	(%)	s^{-1}	(%)	s^{-1}	(%)	μM	(%)	μM	(%)
Wild type	0.149	2.26	0.184	(100)	0.270	(100)	0.0250	(100)	0.144	(100)	3.2	(100)	6.7	(100)
S186A	0.181	1.76	0.194	(106)	—[b]		0.0034	(14)	0.590	(410)	5.2	(162)	8.3	(124)
S186E	0.127	1.84	0.254	(139)	0.184	(68)	0.0159	(64)	0.119	(83)	2.2	(68)	4.3	(64)
E439A	0.172	2.00	0.174	(95)	—[b]		0.0067	(27)	0.452	(314)	6.7	(217)	6.2	(92)
E439S	0.142	1.86	0.250	(136)	—[b]		0.0121	(49)	0.306	(213)	8.7	(273)	13.4	(200)
S186A/E439A	0.154	1.78	0.116	(63)	—[b]		0.0052	(21)	0.491	(341)	5.4	(169)	6.6	(99)
S186E/E439S	0.146	1.64	0.363	(198)	0.185	(68)	0.0221	(89)	0.261	(181)	3.5	(110)	5.9	(88)

[a] The rate most likely reflects the rate-limiting *E*1PCa$_2$ to *E*2P transition in step 4 in the presence of 0.1 M K^+.
[b] Not determined because *E*2P was not accumulated.

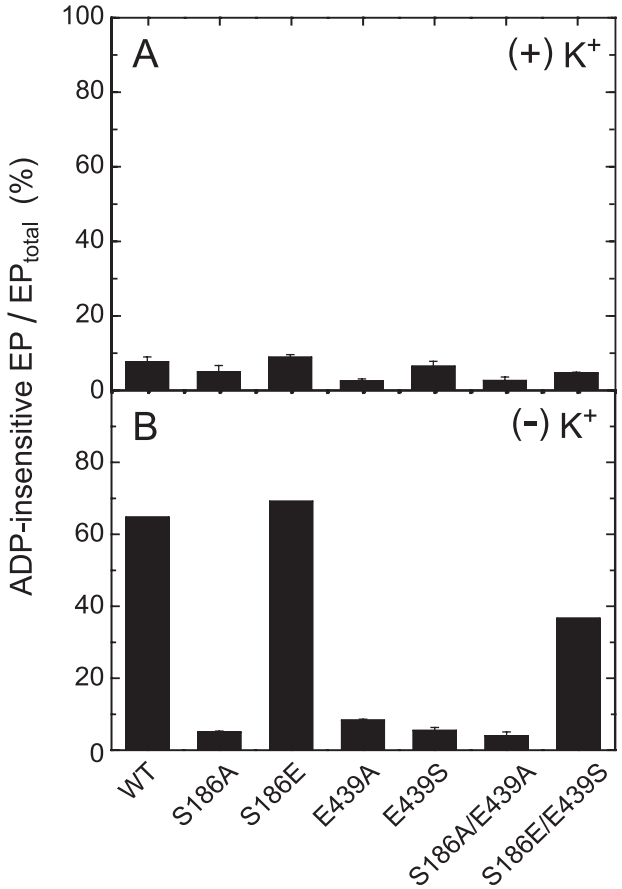

FIGURE 4. **Accumulation of ADP-insensitive *E*P in the presence (*A*) and absence (*B*) of K^+.** Microsomes expressing the wild type or mutant were phosphorylated with 10 μM [γ-^{32}P]ATP at 0 °C for 15 s in 50 μl of a mixture containing 2.5 μg of microsomal protein, 1 μM A23187, 7 mM $MgCl_2$, 0.05 mM $CaCl_2$, 50 mM MOPS/Tris (pH 7.0), and 0.1 M KCl (*A*) or 0.1 M LiCl without KCl (*B*). The total amount of *E*P formed was determined by the acid-quenching. For determination of ADP-insensitive *E*P (*E*2P), an equal volume of a mixture containing 10 mM ADP, 7 mM $MgCl_2$, 10 mM EGTA, 50 mM MOPS/Tris (pH 7.0), and 0.1 M KCl (*A*) or LiCl without KCl (*B*) was added to the above phosphorylation mixture, and the reaction was quenched at 1 s after the ADP addition. ADP-sensitive *E*P (*E*1PCa_2) disappeared entirely within 1 s after the ADP addition. The amount of *E*2P is shown as percentage of the total amount of *E*P.

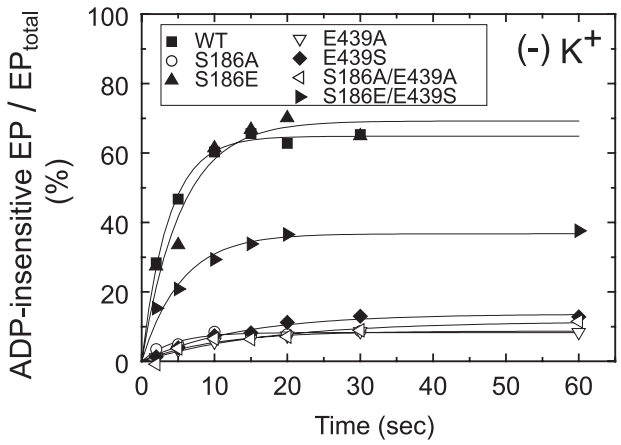

FIGURE 5. **Time course of accumulation of ADP-insensitive *E*P from *E*1Ca_2 and ATP.** Microsomes expressing the wild type or mutant were phosphorylated with [γ-^{32}P]ATP at 0 °C for various periods in the presence of 0.1 M LiCl without KCl otherwise as in Fig. 4*B*. The total amount of *E*P and the amount of ADP-insensitive *E*P (*E*2P) were determined at the indicated time without and with the ADP addition in 0.1 M LiCl (no KCl), otherwise as in Fig. 4*B*. *Solid lines* show the least squares fit to a single exponential, and the apparent rates to reach the steady-state *E*2P level are given in Table 1.

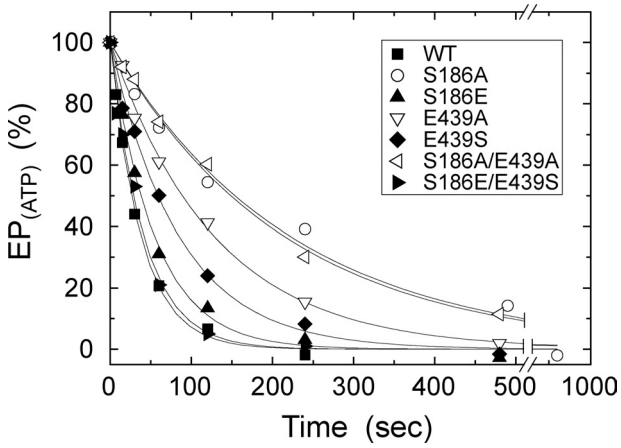

FIGURE 6. **Decay of *E*1PCa_2 formed from ATP.** Microsomes expressing the wild type or mutant were phosphorylated in 0.1 M KCl at 0 °C for 15 s as in Fig. 4*A*. Phosphorylation was terminated by addition of an equal volume of a buffer containing 8 mM EGTA, 0.1 M KCl, 7 mM $MgCl_2$, and 50 mM MOPS/Tris (pH 7.0) at 0 °C. The total amount of *E*P remaining after the EGTA addition was determined at the indicated time. The total amounts of *E*P obtained at zero time (*i.e.* immediately before the EGTA addition) are normalized to 100%. *Solid lines* show the least squares fit to a single exponential, and the decay rates obtained are given in Table 1.

accumulation largely increased in the wild type, S186E, and S186E/E439S. By contrast, the *E*2P accumulation in S186A, E439A, E439S, and S186A/E439A was very low even in the absence of K^+, therefore the *E*1PCa_2 to *E*2P isomerization was likely retarded and/or the *E*2P hydrolysis was accelerated in these mutants.

In Fig. 5, the time course of *E*2P accumulation upon the addition of ATP to *E*1Ca_2 was determined in the absence of K^+. The total amount of *E*P reached its maximum level very rapidly (within ~1 s) and remained unchanged during the period of observation and therefore the time course actually reflects the accumulation of *E*2P from *E*1PCa_2. The *E*2P accumulation proceeded with first-order kinetics, and the rates obtained are listed in Table 1. The rates in the mutants S186E and S186E/E439S were only slightly slowed. In S186A, E439A, S186A/E439A, and E439S, *E*2P was not accumulated.

For the analysis of the *E*1PCa_2 to *E*2P isomerization in the presence of K^+, *E*1PCa_2 was first accumulated with ATP and its decay time course was determined in Fig. 6. This is because, as well known with the wild type (44), the *E*1PCa_2 decay reflects the rate-limiting *E*1PCa_2 to *E*2P isomerization followed by the rapid *E*2P hydrolysis. In fact, almost all of *E*P present at each time point was *E*1PCa_2 in the mutants as well as in the wild type (data not shown, but see Fig. 4*A*). The decay time courses were well fitted with a single exponential, and the rates obtained are listed in Table 1. In S186A, E439A, and S186A/E439A, the decay rate was markedly reduced to 14~27% of the wild type. The rate was also reduced significantly in E439S and to some extent in S186E. In the swap mutant S186E/E439S, the wild-type rate was almost restored.

Hydrolysis of E2P Formed from P_i—The *E*2P hydrolysis was examined by first phosphorylating the enzyme with $^{32}P_i$ in the absence of Ca^{2+} and K^+ and presence of 35% (v/v) Me_2SO, which extremely favors *E*2P formation (45), and then by dilut-

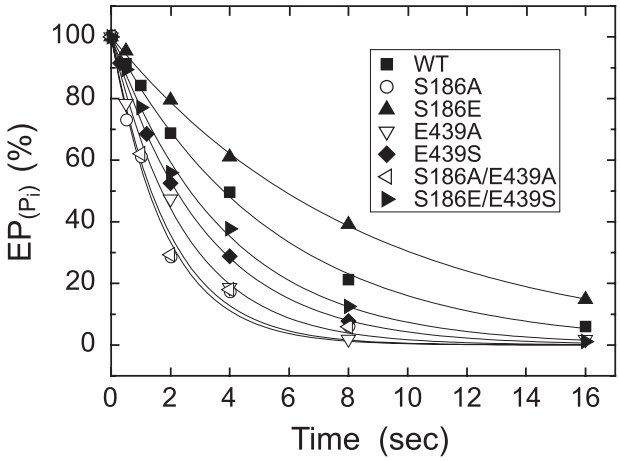

FIGURE 7. **Hydrolysis of *E*2P formed from P_i without Ca^{2+}.** Microsomes expressing the wild type or mutant were phosphorylated with 0.1 mM $^{32}P_i$ at 25 °C for 10 min in 5 μl of a mixture containing 2 μg of microsomal protein, 20 μM A23187, 1 mM EGTA, 7 mM $MgCl_2$, 50 mM MOPS/Tris (pH 7.0), and 35% (v/v) Me_2SO. The mixture was then cooled and diluted at 0 °C by 100 μl of a mixture containing 1.05 mM non-radioactive P_i, 105 mM KCl, 15.8 mM EGTA, and 50 mM MOPS/Tris (pH 7.0). At different times after the dilution, the *E*2P hydrolysis was quenched by acid. The amounts of *E*2P formed with $^{32}P_i$ at zero time are normalized to 100%. *Solid lines* show the least squares fit to a single exponential, and the rates obtained are given in Table 1.

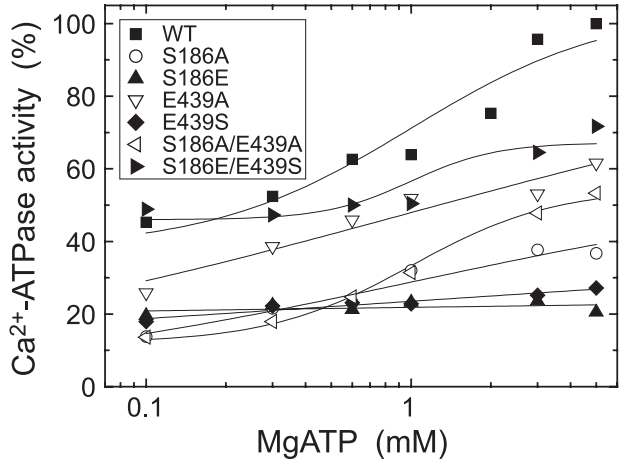

FIGURE 8. **MgATP dependence of Ca^{2+}-ATPase activity.** The Ca^{2+}-ATPase activity of microsomes expressing the wild type or mutant was determined at various concentrations of [γ-^{32}P]ATP otherwise as in Fig. 3. Almost all of ATP (more than 97% of total ATP) is in MgATP. The activities of the mutants are presented as a percentage of that of the wild type at 5 mM MgATP.

ing the phosphorylated samples at 0 °C with a large volume of solution containing non-radioactive P_i and K^+ without Ca^{2+} (Fig. 7). The conditions were thus made otherwise the same as those for the decay of *E*1PCa_2 formed from ATP (*E*1PCa_2 to *E*2P isomerization) in Fig. 6. Hydrolysis of ^{32}P-labeled *E*2P proceeded with first-order kinetics, and the rates obtained are listed in Table 1. As compared with the wild type, the rate was markedly increased in the alanine mutants S186A, E439A, S186A/E439A, and also in E439S at a lower extent. The result of E439A is consistent with the previous observation by Clausen *et al.* (29). The rate was slightly decreased in S186E, in contrast to the marked increase in S186A and the Darier disease mutant S186F of SERCA2b (30). The swap mutant S186E/E439S exhibited an intermediate rate between those of E439S and S186E, and thus brought the markedly increased rate of E439S toward the wild-type one.

Note that the overall Ca^{2+}-ATPase activity was significantly inhibited in all the alanine mutants, S186E, and E439S, despite the markedly accelerated *E*2P hydrolysis (or unretarded hydrolysis in S186E). Therefore, the inhibition of the Ca^{2+}-ATPase activity in the mutants is ascribed to the retardation of the rate-limiting *E*1PCa_2 to *E*2P isomerization.

BeF_3^- and AlF_4^- Affinities in Formation of E2·BeF_3^- and E2·AlF_4^-—The *E*2 state Ca^{2+}-ATPase in the absence of Ca^{2+} forms the complexes *E*2·BeF_3^- and *E*2·AlF_4^-, which are analogs of the *E*2P ground state and of the transition state of the *E*2P hydrolysis, respectively (22). In supplemental Fig. S3 and Table 1, the effects of the mutations on the affinities for BeF_3^- and AlF_4^- were determined by changing the beryllium and aluminum concentrations in the presence of excess 2 mM fluoride and by determining the inhibition of *E*P formation from ATP. In the *E*2·BeF_3^- formation, the mutations S186A, E439A, S186A/E439A, and E439S significantly decreased the BeF_3^- affinity, S186E increased slightly, and the swap mutation S186E/E439S restored the wild-type affinity. In the *E*2·AlF_4^- formation, the mutation effects were much less pronounced or not exhibited. The results agree with the mutation effects on the *E*2P hydrolysis (Fig. 7) that the alanine mutations and E439S markedly enhance the hydrolysis rate, S186E reduces slightly, and the swap mutation S186E/E439A restores the wild-type rate. The results indicated that the hydrogen-bonding interaction between Ser^{186} and Glu^{439} functions to stabilize the *E*2P ground state.

Modulatory MgATP-induced Acceleration of Ca^{2+}-ATPase Activity—As known for a long time (46), the Ca^{2+}-ATPase activity of the wild type is markedly increased by MgATP at sub-mM ~ mM range. This modulatory MgATP effect was examined at various MgATP concentrations in Fig. 8. The mutants S186A, E439A, and S186A/E439A exhibited the marked increase with increasing MgATP concentration despite their significantly reduced activity at the low ATP concentrations (see Fig. 3). The result on E439A is consistent with the previous observation by Clausen *et al.* (29). The activity was increased only slightly in E439S with MgATP and not increased at all in S186E. In the swap mutant S186E/E439S, the activity was increased with MgATP, and thus the MgATP modulatory effect as well as the activity was almost restored. In Figs. 9–11, the modulation by MgATP and free ATP was further explored in each of the steps; the *E*1PCa_2 to *E*2P isomerization and the *E*2P hydrolysis.

Modulatory MgATP- and ATP-induced Acceleration of E1PCa_2 to E2P Isomerization—*E*1PCa_2 was first formed with 10 μM MgATP in the presence of K^+ under conditions in which *E*1PCa_2 accumulates dominantly (see Fig. 4*A*). Then, the MgATP modulation of the *E*1PCa_2 decay (the rate-limiting *E*1PCa_2 to *E*2P isomerization) was examined by the subsequent addition of various concentrations of MgATP together with an excess EGTA to remove free Ca^{2+}. The decay time courses were fitted well with a single exponential (data not shown). In Fig. 9, the rates thus determined are plotted *versus* the MgATP concentration. The values V_0 (the rate at 10 μM MgATP), V_{max} (the maximum rate at a saturating MgATP concentration), and $K_{0.5}$ (giving the half-maximum rate) are obtained by fitting the

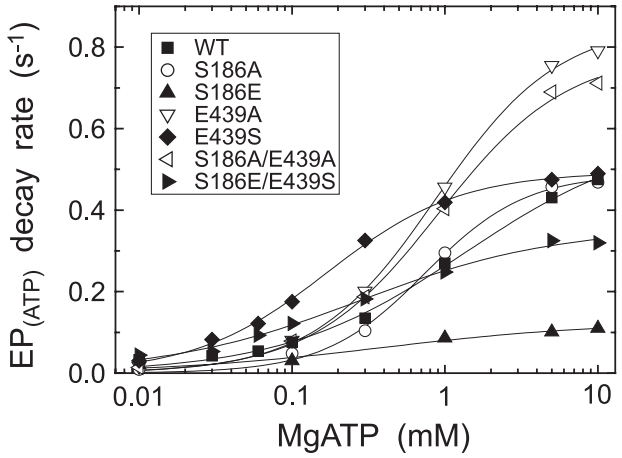

FIGURE 9. **MgATP dependence of the decay rate of *E*1PCa$_2$ formed from ATP.** *E*1PCa$_2$ was first formed in 50 μl of a microsomes suspension in 10 μM [γ-^{32}P]ATP, 10 μM Ca^{2+} (0.98 mM $CaCl_2$ with 1 mM EGTA), and 0.1 M KCl, otherwise as in Fig. 4*A*. Phosphorylation was terminated by 100 μl of a buffer containing 8 mM EGTA, 1 μM A23187, 0.1 M KCl, 50 mM MOPS/Tris (pH 7.0), and various concentrations of ATP and $MgCl_2$ (producing MgATP (more than 97% of the total ATP) with 6.2 mM free Mg^{2+}). At different times after this MgATP addition, the decay reaction of *E*1PCa$_2$ at 0 °C was quenched by acid. The rate of the single exponential decay of *E*1PCa$_2$ obtained was plotted *versus* the MgATP concentration. *Solid lines* show the least squares fit to the Hill equation, and the parameters V_0 (the rate at the lowest 10 μM MgATP), V_{max} (the maximum rate), and $K_{0.5}$ (MgATP concentration giving the half-maximal change) are given in Table 2.

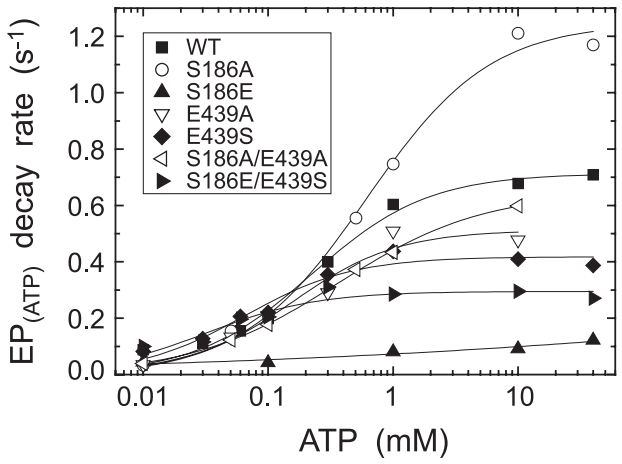

FIGURE 10. **ATP dependence of the decay rate of *E*1PCa$_2$ formed from ATP.** The *E*1PCa$_2$ decay was followed after addition of various concentrations of ATP and 30 mM EDTA without $MgCl_2$ (in place of 8 mM EGTA) otherwise as in Fig. 9. The single exponential decay rate of *E*1PCa$_2$ obtained was plotted *versus* the metal-free ATP concentration, and the parameters V_0, V_{max}, and $K_{0.5}$ estimated as in Fig. 9 are given in Table 2.

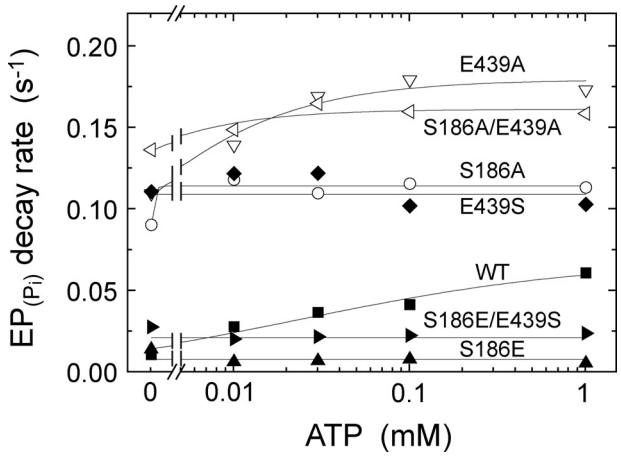

FIGURE 11. **ATP dependence of the rate of *E*2P hydrolysis.** Microsomes expressing the wild type or mutant were phosphorylated with $^{32}P_i$ at 25 °C for 10 min in 4 μl of a mixture containing 1.6 μg of microsomal protein, 0.1 mM $^{32}P_i$, 20 μM A23187, 1 mM EGTA, 7 mM $MgCl_2$, 50 mM MOPS/Tris (pH 7.0), and 35% (v/v) Me_2SO. The mixture was then diluted at 0 °C by addition of 196 μl of a mixture containing 1.02 mM non-radioactive P_i, 50 mM MOPS/Tris (pH 7.0), 15.3 mM EDTA, and various concentration of ATP. At different times after the dilution, the *E*2P hydrolysis was quenched by acid. The rate of the single exponential *E*2P hydrolysis was plotted *versus* the ATP concentration, and the parameters V_0 (the rate without ATP), V_{max} (the rate at the highest ATP concentration, 1 mM), and $K_{0.5}$ (ATP concentration giving the half-maximal change) are given in Table 2. It should be noted that Mg^{2+} bound at the catalytic site of *E*2P is occluded (53), and therefore the *E*2P hydrolysis takes place even after removal of free Mg^{2+}.

curves to the Hill equation and shown in Table 2. In the wild-type, MgATP enhanced the *E*P isomerization rate by 18-fold (V_{max}/V_0) with $K_{0.5}$ of 1.35 mM. In the alanine mutants S186A, E439A, and S186A/E439A, the magnitudes of MgATP-induced acceleration were much larger (54-, 50-, and 56-fold, respectively) with slightly higher MgATP affinities than the wild type. In E439S and the swap mutant S186E/E439S, the magnitudes of MgATP-induced acceleration were similar to or somewhat smaller than the wild type (16.5- and 8.3-fold, respectively) and their MgATP affinities were markedly higher than the wild type. In S186E, the MgATP-induced acceleration was least (5.5-fold), and consequently, the rate in this mutant at the high MgATP concentrations, *e.g.* at 10 mM became much lower than the wild type. Note that this markedly reduced rate in S186E was increased by the swap mutation S186E/E439S to the significant level close to the wild type.

The modulatory effect of metal-free ATP on the *E*P isomerization was also explored, in this case, by adding various concentrations of ATP together with an excess EDTA to remove free Ca^{2+} and Mg^{2+} (Fig. 10). The *E*1PCa$_2$ decay time courses of the wild type and mutants were apparently fitted to a single exponential kinetics but not strictly (data not shown). This complicated kinetics may be because Mg^{2+} bound at the catalytic site was likely removed by the added EDTA in some *E*1PCa$_2$ fraction as previously also noted (29). Nevertheless, for simplicity, the single exponential rates estimated were plotted in Fig. 10. The parameters $K_{0.5}$, V_0 (at 10 μM ATP), V_{max} in the ATP dependence curve are listed in Table 2.

In the wild type, the affinity of metal-free ATP for the modulation was significantly higher than that of MgATP (29); thus Mg^{2+} in MgATP brings its modulatory binding to correspond to cellular level of ATP (mostly MgATP complex). In the alanine mutants S186A, E439A, and S186A/E439A (most profoundly in S186A), the increase in free ATP concentration from 0.01 to 40 mM exhibited the marked acceleration of the *E*1PCa$_2$ decay by 38-, 15-, and 17-fold, respectively, which are even much more than that of the wild type (8-fold). The free ATP affinities in the alanine mutants were similar to and not higher than the wild type. The results of E439A are in agreement with the previous study by Clausen *et al.* (29).

In E439S, the extent of the acceleration was 5.1-fold and slightly smaller than that of the wild type with somewhat increased ATP affinity. In S186E, the ATP-induced acceleration of *E*P isomerization was very small (2.7-fold), and actually

TABLE 2

Parameters determined for the MgATP/ATP-induced acceleration of partial reaction steps

The modulatory MgATP- and metal-free ATP-induced acceleration of the decay rate of EP$_{ATP}$ formed from ATP and Ca^{2+} (*i.e.* the rate-limiting E1PCa_2 to E2P isomerization) and that of the hydrolysis of E2P$_{Pi}$ formed from P_i in the absence of Ca^{2+} were determined as described in Figs. 9–11. The kinetic parameters in the nucleotide dependence curves were obtained by the fitting to the Hill equation in Figs. 9 and 10, or roughly by the eye inspection in Fig. 11; $K_{0.5}$ (the MgATP or ATP concentration giving the half-maximum acceleration), V_0 (the rate at 10 μM MgATP or ATP in Figs. 9 and 10, and no ATP in Fig. 11), and V_{max} (the maximum rate in Figs. 9 and 10, or the rate at the highest 1 mM ATP in Fig. 11).

	MgATP dependence of EP$_{ATP}$ decay			ATP dependence of EP$_{ATP}$ decay			ATP dependence of E2P$_{Pi}$ hydrolysis		
	(+)Mg^{2+}			(−)Mg^{2+}			(−)Mg^{2+}		
	$K_{0.5}$	V_0	V_{max}	$K_{0.5}$	V_0	V_{max}	$K_{0.5}$	V_0 (no ATP)	V_{max} (1 mM ATP)
	mM	s^{-1}	s^{-1}	mM	s^{-1}	s^{-1}	μM	s^{-1}	s^{-1}
Wild type	1.351	0.033	0.591	0.224	0.088	0.714	60	0.016	0.066
S186A	0.738	0.009	0.489	0.612	0.033	1.248	—[a]	0.095	0.118
S186E	—[a]	0.020	0.110[b]	—[a]	0.045	0.121[c]	—[a]	0.019	0.010
E439A	0.874	0.017	0.857	0.155	0.035	0.513	10	0.115	0.178
E439S	0.170	0.030	0.494	0.065	0.082	0.418	—[a]	0.116	0.108
S186A/E439A	0.913	0.014	0.786	0.360	0.039	0.647	12	0.141	0.164
S186E/E439S	0.281	0.043	0.357	0.032	0.010	0.295	—[a]	0.033	0.029

[a] Not determined.
[b] The value at the highest (10 mM) ATP.
[c] The value at the highest (40 mM) ATP.

at the highest 40 mM ATP, the isomerization rate was only 17% of the wild-type rate. However, in the swap mutation S186E/E439S, the marked ATP-induced acceleration (by 30-fold) was restored with the ATP affinity much higher than the wild type.

ATP Modulation of E2P Hydrolysis—The modulation of the E2P hydrolysis was examined only with metal-free ATP, because metal-free ATP but not MgATP is able to bind to E2P for the modulation with a reasonable affinity (47, 48). E2P was first formed by $^{32}P_i$ in the absence of Ca^{2+} and K^+ and presence of Me_2SO as in Fig. 7, then the phosphorylated sample was largely diluted with a buffer containing excess EDTA and various concentrations of ATP, and the E2P hydrolysis was followed in the absence of K^+ (in the presence of K^+, the hydrolysis especially at high ATP was too fast to be followed). In Fig. 11, the single exponential rates of E2P hydrolysis were plotted *versus* the ATP concentration. In the absence of K^+ without ATP, the hydrolysis rate (V_0 in Table 2) was significantly faster in the mutants S186A, E439A, S186A/E439A, and E439S than in the wild type, as was found in the presence of K^+ without ATP (Fig. 7 and Table 1). The V_0 of S186E was similar to that of the wild type, and the swap mutant S186E/E439S exhibited the intermediate V_0 value between S186E and E439S; thus, restored almost the wild-type rate from the markedly enhanced one in E439S.

With increasing ATP to 1 mM, the hydrolysis rate in the wild type increased by 4.1-fold. In S186E and in S186E/E439S, the rate was not increased or rather decreased slightly by 1 mM ATP; therefore, the swap mutation did not restore the ATP modulation. No ATP acceleration was found with E439S, although its rate was markedly elevated as compared with the wild type. In E439A, S186A, and S186A/E439A, the markedly elevated rates without ATP were slightly increased with increasing ATP by 1.2~1.5-fold.

DISCUSSION

Roles of Ser^{186}-Glu^{439} Interactions in E1PCa_2 to E2P Isomerization and E2P Hydrolysis in the Absence of Modulatory ATP—In the absence of modulatory ATP, we observed here that the substitutions of Ser^{186} and Glu^{439}, especially by alanine(s) S186A, E439A, and S186A/E439A result in the markedly retarded E1PCa_2 to E2P isomerization and markedly accelerated E2P hydrolysis. Such changes were also found in E439S and S186E with a somewhat less extent (in S186E the change was only the retardation of the EP isomerization). Most importantly, these changes as well as the inhibition of the overall Ca^{2+}-ATPase activity were almost relieved by the swap mutation S186E/E439S, and thus the wild-type properties were restored. The results demonstrated that the Ser^{186}-Glu^{439} hydrogen bond between the A and N domains functions to stabilize the E2P structure, consistent with the prediction made with the mutation E439A (29). The loss of the Ser^{186}-Glu^{439} interdomain interaction destabilized the E2P structure. In theory, the transition state structure is close to the product state (*e.g.* see the textbook by Fersht, Ref. 49); therefore, the transition state of the E1PCa_2 to E2P isomerization is probably also destabilized by the loss of the interaction causing the retardation of EP isomerization.

Note in Table 1 that the disruption of the Ser^{186}-Glu^{439} hydrogen bond by the mutations caused the reduction of the BeF_3^- affinity for the E2·BeF_3^- formation concomitantly with the marked acceleration of the E2P hydrolysis, and that the swap mutation S186E/E439S restored the wild type properties. The results obviously show that the E2P ground state is stabilized by the Ser^{186}-Glu^{439} hydrogen bond. This interaction therefore functions to retard the catalytic structural events, which involve rearrangement of the catalytic site for the attack of the TGES^{184}-coordinated specific water on the Asp^{351}-acylphosphate. The E2P stabilization may be important to avoid the too (un-physiologically) rapid E2P hydrolysis, and thereby making the resident time of E2P long enough for Ca^{2+}-release (E2PCa_2 → E2P + $2Ca^{2+}$) and preventing a possible E2PCa_2 hydrolysis without Ca^{2+}-release for the energy coupling.

Regarding the positioning of the TGES^{184} loop, the A domain largely rotates for the E1PCa_2 to E2P isomerization and its outermost TGES^{184} comes above the Asp^{351} region of the P domain; therefore blocking the access of the ADP β-phosphate

to Asp^{351}-acylphosphate. For the subsequent acylphosphate hydrolysis, the rearrangement in the catalytic site takes place so as to produce the appropriate positioning of the TGES^{184} loop with the coordinated attacking water molecule. Because Ser^{186} is situated in the immediate C terminus of TGES^{184}, it is likely that the Ser^{186}-Glu^{439} hydrogen bond in *E*2P may be stabilizing the TGES^{184} loop at the position after the loss of the ADP sensitivity but before gaining the catalytic activity for the Asp^{351}-acylphosphate hydrolysis. Then, during the rearrangement of the catalytic site structure via the transition state for the hydrolysis, $E2P + H_2O \rightarrow E2 + P_i$, the Ser^{186}-Glu^{439} hydrogen bond would be lost.

In the crystal structures of $E2{\cdot}BeF_3^-$ (*E*2P ground state), Ser^{186} and Glu^{439} are actually closely located (2.5–2.8 Å) with their hydrogen bond, whereas in $E2{\cdot}AlF_4^-$ (transition state of *E*2P hydrolysis) they are more separated (2.9–3.4 Å) (15, 18, 19). In the *E*2(TG) structures, the two residues are far more separated (~10 Å). The loss of the Ser^{186}-Glu^{439} interaction is of course associated with the motions and separation of the cytoplasmic domains A, N, and P. Such rearrangement is actually reflected by the change in the catalytic site from the strongly hydrophobic closed structure in the *E*2P ground state to the hydrophilic opened one in the transition state and product $E2{\cdot}P_i$ state as well as in the *E*2 state (22).

We examined the structure of the mutants S186E/E439S, S186E, and E439S with the crystal structures $E2{\cdot}BeF_3^-$, 2ZBE (18) and 3B9B (19) by the program Swiss-PdbViewer (50). The structural modeling of the mutants actually agreed with their kinetic consequences and with the predicted roles of the Ser^{186}-Glu^{439} hydrogen-bonding interaction in the *E*P processing (*i.e.* marked effects by the alanine mutations, smaller effects in E439S, and further smaller effects in S186E, and the restoration in S186E/E439S). Namely, in S186E/E439S, the two introduced residues are able to produce their hydrogen bond as in the wild type. In S186E, the introduced glutamate is still potentially able to produce a hydrogen bond with the partner residue Glu^{439}. In this case, pK_a of the introduced glutamate was estimated by ProPKa (51) to become extremely high, 7.61 (2ZBE) or 9.20 (3B9B); therefore, it is protonated thus avoiding repulsion with Glu^{439}. In E439S, the introduced small serine may not reach the partner residue (Ser^{186}) but possibly produces a polar interaction. In the alanine mutants, the introduced non-polar small alanine(s) at the position(s) of Ser^{186} and Glu^{439} is obviously not able to produce a hydrogen bond.

Ser^{186}-Glu^{439} Interaction in ATP Modulation of EP Processing—The retarded $E1PCa_2$ to *E*2P isomerization in the alanine mutants S186A, E439A, and S186A/E439A was markedly accelerated with increasing ATP/MgATP, and the isomerization became even faster in some mutants than in the wild type at high ATP/MgATP concentrations. Thus the modulatory ATP/MgATP binding overcame the mutation-induced destabilization of *E*2P structure. Results indicate that Ser^{186} and Glu^{439} are not involved directly in the modulatory ATP/MgATP binding for the $E1PCa_2$ to *E*2P isomerization. Results also show that formation of both the Ser^{186}-Glu^{439} interdomain hydrogen bond and the structure needed for the modulatory ATP/MgATP binding occurs upon the $E1PCa_2$ to *E*2P isomerization, in which the A, N, and P domains gather to form the most compactly organized state. The necessity for a close interaction between the A and N domains was recently supported by the observation (52) that the residues of the A domain Arg^{174}, Ile^{188}, and Lys^{205} are involved in the binding of modulatory ATP/MgATP in the *E*2P state. Our mutations further showed that S186E disrupts seriously the modulatory ATP/MgATP acceleration of the $E1PCa_2$ to *E*2P isomerization, and that the swap mutation S186E/E439S restores almost the wild-type acceleration. The introduced long and negatively charged glutamate in S186E likely caused a steric collision (repulsion) with the modulatory ATP/MgATP thus inhibiting the modulation. In S186E/E439S, the hydrogen bond between the introduced two residues probably fixed the glutamate configuration of S186E; thereby avoided its inhibitory effect and restored the ATP/MgATP modulation of the *E*P isomerization. Notably, the affinities of S186E/E439S and E439S for the modulatory ATP and MgATP in the *E*P isomerization were significantly higher than those of the wild type (see Table 2), indicating the importance of the Ser^{186}-Glu^{439} hydrogen bond in the affinity of the modulatory MgATP (ATP) suitable to its cellular level.

In S186E, the ATP modulation of the *E*2P hydrolysis was also lost. The swap mutation S186E/E439S did not restore it, in contrast to the restored modulation of the $E1PCa_2$ to *E*2P isomerization. Results show that the structure of the modulatory ATP binding site and/or configuration of ATP for the $E1PCa_2$ to *E*2P isomerization are distinct from those for the *E*2P hydrolysis; therefore altered for (during) the *E*2P hydrolysis. This agrees with the fact that the *E*2P hydrolysis involves separation of the N, A, and P domains to the more loosely organized state in *E*2. Actually, in *E*2(TG)AMPPCP structure, Ser^{186} is far from Glu^{439} and ATP (10~13 Å), and Glu^{439} participates in binding of the ATP phosphate moiety via Mg^{2+} (16). In $E2{\cdot}AlF_4^-$ with bound AMPPCP, Ser^{186} is still close to Glu^{439} and the bound modulatory ATP (AMPPCP α-phosphate). The modulatory ATP likely accelerates the release of the A domain (Ser^{186}) from the N domain (Glu^{439}). As Glu^{439} becomes involved in the modulatory ATP binding during the *E*2P hydrolysis to *E*2, the swap mutation S186E/E439S did not restore the ATP modulation of the *E*2P hydrolysis that is disrupted in S186E.

Acknowledgments—We thank Dr. David H. MacLennan, University of Toronto, for the generous gift of SERCA1a cDNA and Dr. Randal J. Kaufman, Genetics Institute, Cambridge, MA, for the generous gift of the expression vector pMT2. We are also grateful to Dr. Chikashi Toyoshima, University of Tokyo, for helpful discussions.

REFERENCES

1. Hasselbach, W., and Makinose, M. (1961) *Biochem. Z.* **333,** 518–528
2. Ebashi, S., and Lipmann, F. (1962) *J. Cell Biol.* **14,** 389–400
3. Inesi, G., Sumbilla, C., and Kirtley, M. E. (1990) *Physiol. Rev.* **70,** 749–760
4. Møller, J. V., Juul, B., and le Maire, M. (1996) *Biochim. Biophys. Acta* **1286,** 1–51
5. MacLennan, D. H., Rice, W. J., and Green, N. M. (1997) *J. Biol. Chem.* **272,** 28815–28818
6. McIntosh, D. B. (1998) *Adv. Mol. Cell. Biol.* **23,** 33–99
7. Toyoshima, C., and Inesi, G. (2004) *Annu. Rev. Biochem.* **73,** 269–292
8. Toyoshima, C. (2008) *Arch. Biochem. Biophys.* **476,** 3–11
9. Toyoshima, C. (2009) *Biochim. Biophys. Acta* **1793,** 941–946
10. Toyoshima, C., Nakasako, M., Nomura, H., and Ogawa, H. (2000) *Nature*

405, 647–655
11. Toyoshima, C., and Nomura, H. (2002) *Nature* **418,** 605–611
12. Sørensen, T. L.-M., Møller, J. V., and Nissen, P. (2004) *Science* **304,** 1672–1675
13. Toyoshima, C., and Mizutani, T. (2004) *Nature* **430,** 529–535
14. Toyoshima, C., Nomura, H., and Tsuda, T. (2004) *Nature* **432,** 361–368
15. Olesen, C., Sørensen, T. L., Nielsen, R. C., Møller, J. V., and Nissen, P. (2004) *Science* **306,** 2251–2255
16. Jensen, A. M., Sørensen, T. L., Olesen, C., Møller, J. V., and Nissen, P. (2006) *EMBO J.* **25,** 2305–2314
17. Takahashi, M., Kondou, Y., and Toyoshima, C. (2007) *Proc. Natl. Acad. Sci. U.S.A.* **104,** 5800–5805
18. Toyoshima, C., Norimatsu, Y., Iwasawa, S., Tsuda, T., and Ogawa, H. (2007) *Proc. Natl. Acad. Sci. U.S.A.* **104,** 19831–19836
19. Olesen, C., Picard, M., Winther, A. M., Gyrup, C., Morth, J. P., Oxvig, C., Møller, J. V., and Nissen, P. (2007) *Nature* **450,** 1036–1042
20. Danko, S., Daiho, T., Yamasaki, K., Kamidochi, M., Suzuki, H., and Toyoshima, C. (2001) *FEBS Lett.* **489,** 277–282
21. Danko, S., Yamasaki, K., Daiho, T., Suzuki, H., and Toyoshima, C. (2001) *FEBS Lett.* **505,** 129–135
22. Danko, S., Yamasaki, K., Daiho, T., and Suzuki, H. (2004) *J. Biol. Chem.* **279,** 14991–14998
23. Kato, S., Kamidochi, M., Daiho, T., Yamasaki, K., Gouli, W., and Suzuki, H. (2003) *J. Biol. Chem.* **278,** 9624–9629
24. Yamasaki, K., Daiho, T., Danko, S., and Suzuki, H. (2004) *J. Biol. Chem.* **279,** 2202–2210
25. Wang, G., Yamasaki, K., Daiho, T., and Suzuki, H. (2005) *J. Biol. Chem.* **280,** 26508–26516
26. Yamasaki, K., Wang, G., Daiho, T., Danko, S., and Suzuki, H. (2008) *J. Biol. Chem.* **283,** 29144–29155
27. Daiho, T., Yamasaki, K., Wang, G., Danko, S., Iizuka, H., and Suzuki, H. (2003) *J. Biol. Chem.* **278,** 39197–39204
28. Daiho, T., Yamasaki, K., Danko, S., and Suzuki, H. (2007) *J. Biol. Chem.* **282,** 34429–34447
29. Clausen, J. D., McIntosh, D. B., Anthonisen, A. N., Woolley, D. G., Vilsen, B., and Andersen, J. P. (2007) *J. Biol. Chem.* **282,** 20686–20697
30. Dode, L., Andersen, J. P., Leslie, N., Dhitavat, J., Vilsen, B., and Hovnanian, A. (2003) *J. Biol. Chem.* **278,** 47877–47889
31. Miyauchi, Y., Daiho, T., Yamasaki, K., Takahashi, H., Ishida-Yamamoto, A., Danko, S., Suzuki, H., and Iizuka, H. (2006) *J. Biol. Chem.* **281,** 22882–22895
32. Ma, H., Inesi, G., and Toyoshima, C. (2003) *J. Biol. Chem.* **278,** 28938–28943
33. Inesi, G., Ma, H., Lewis, D., and Xu, C. (2004) *J. Biol. Chem.* **279,** 31629–31637
34. Kaufman, R. J., Davies, M. V., Pathak, V. K., and Hershey, J. W. B. (1989) *Mol. Cell. Biol.* **9,** 946–958
35. Maruyama, K., and MacLennan, D. H. (1988) *Proc. Natl. Acad. Sci. U.S.A.* **85,** 3314–3318
36. Daiho, T., Yamasaki, K., Suzuki, H., Saino, T., and Kanazawa, T. (1999) *J. Biol. Chem.* **274,** 23910–23915
37. Kanazawa, T., Saito, M., and Tonomura, Y. (1970) *J. Biochem.* **67,** 693–711
38. Weber, K., and Osborn, M. (1969) *J. Biol. Chem.* **244,** 4406–4412
39. Daiho, T., Suzuki, H., Yamasaki, K., Saino, T., and Kanazawa, T. (1999) *FEBS Lett.* **444,** 54–58
40. Lowry, O. H., Rosebrough, N. J., Farr, A. L., and Randall, R. J. (1951) *J. Biol. Chem.* **193,** 265–275
41. Humphrey, W., Dalke, A., and Schulten, K. (1996) *J. Mol. Graph.* **14,** 33–38, 27–28
42. Pick, U., and Karlish, S. J. D. (1982) *J. Biol. Chem.* **257,** 6120–6126
43. Shigekawa, M., and Pearl, L. J. (1976) *J. Biol. Chem.* **251,** 6947–6952
44. Shigekawa, M., and Dougherty, J. P. (1978) *J. Biol. Chem.* **253,** 1451–1457
45. de, Meis, L., and Inesi, G. (1982) *J. Biol. Chem.* **257,** 1289–1294
46. Yamamoto, T., and Tonomura, Y. (1967) *J. Biochem.* **62,** 558–575
47. Champeil, P., Riollet, S., Orlowski, S., Guillain, F., Seebregts, C. J., and McIntosh, D. B. (1988) *J. Biol. Chem.* **263,** 12288–12294
48. Andersen, J. P., and Møller, J. V. (1985) *Biochim. Biophys. Acta* **815,** 9–15
49. Fersht, A. R. (1999) *Structure and Mechanism in Protein Science: A Guide to Enzyme Catalysis and Protein Folding*, pp. 132–168, W. H. Freeman and Co., New York
50. Guex, N., and Peitsch, M.C. (1997) *Electrophoresis* **18,** 2714–2723
51. Li H., Robertson, A. D., and Jensen, J. H. (2005) *Proteins* **61,** 704–721
52. Clausen, J. D., McIntosh, D. B., Woolley, D. G., and Andersen, J. P. (2008) *J. Biol. Chem.* **283,** 35703–35714
53. Ogurusu, T., Wakabayashi, S., and Shigekawa, M. (1991) *J. Biochem.* **109,** 472–476